NIH Public Access
Author Manuscript
Cell Stem Cell. Author manuscript; available in PMC 2011 April 2.

Published in final edited form as:
Cell Stem Cell. 2010 April 2; 6(4): 323–335. doi:10.1016/j.stem.2010.02.015.

MicroRNA-9 Coordinates Proliferation and Migration of Human Embryonic Stem Cell–Derived Neural Progenitors

Celine Delaloy[1], **Lei Liu**[1], **Jin-A Lee**[1,#], **Hua Su**[2], **Fanxia Shen**[2], **Guo-Yuan Yang**[2], **William L. Young**[2], **Kathy N. Ivey**[3], and **Fen-Biao Gao**[1,4,*]

[1] Gladstone Institute of Neurological Disease and Department of Neurology, University of California, San Francisco, CA 94158, USA

[2] Center for Cerebrovascular Research, Departments of Anesthesia and Perioperative Care and Neurology and Neurosurgery, University of California, San Francisco, CA 94110, USA

[3] Gladstone Institute of Cardiovascular Disease, San Francisco, CA 94158, USA

[4] Department of Neurology, University of Massachusetts Medical School, Worcester, MA 01605, USA

Summary

Human pluripotent stem cells offer promise for use in cell-based therapies for brain injury and diseases. However, their cellular behavior is poorly understood. Here we show that the expression of the brain-specific microRNA-9 (miR-9) is turned on in human neural progenitor cells (hNPCs) derived from human embryonic stem cells. Loss of miR-9 suppressed proliferation but promoted migration of hNPCs cultured in vitro. hNPCs without miR-9 activity also showed enhanced migration when transplanted into mouse embryonic brains or adult brains of a mouse model of stroke. These effects were not due to precocious differentiation of hNPCs. One of the key targets directly regulated by miR-9 encodes stathmin, which increases microtubule instability and whose expression in hNPCs correlates inversely with that of miR-9. Partial inhibition of stathmin activity suppressed the effects of miR-9 loss on proliferation and migration of human or embryonic rat neural progenitors. These results identify miR-9 as a novel regulator that coordinates the proliferation and migration of hNPCs.

Keywords

Human Embryonic Stem Cells; Neural Progenitors; Migration; Proliferation; MicroRNA-9; Stathmin

Introduction

The controlled differentiation of human embryonic stems cells (hESCs) (Hochedlinger and Jaenisch, 2003; Yu and Thomson, 2008), adult (Zhao et al., 2008; Duan et al., 2008) or induced pluripotent stem (iPS) cells (Yamanaka, 2007; Yu and Thomson, 2008) into neural

* Correspondence should be addressed to F.-B.G. (fgao@gladstone.ucsf.edu).
#Present Address: Department of Biotechnology, College of Life Science and Nanotechnology, Hannam University, Dajeon 305-811, Korea.

Publisher's Disclaimer: This is a PDF file of an unedited manuscript that has been accepted for publication. As a service to our customers we are providing this early version of the manuscript. The manuscript will undergo copyediting, typesetting, and review of the resulting proof before it is published in its final citable form. Please note that during the production process errors may be discovered which could affect the content, and all legal disclaimers that apply to the journal pertain.

NIH-PA Author Manuscript
NIH-PA Author Manuscript
NIH-PA Author Manuscript

NIH-PA Author Manuscript

NIH-PA Author Manuscript

NIH-PA Author Manuscript

progenitor cells (NPCs) opens fascinating prospects for cell replacement in injured or diseased brains or spinal cords. The clinical efficacy of grafted progenitor cells critically depends on their ability to migrate to the appropriate sites in the adult central nervous system without unwanted proliferation and tumor formation. However, little is known about the cellular behavior of hNPCs derived from hESCs or how their proliferation and migration are coordinated. Although experiments in rodent models have provided important molecular insights into these cellular processes (e.g. Cobos et al., 2007; Mao et al., 2009), studies performed directly on human cells are of great importance for developing effective therapeutic approaches.

MicroRNAs (miRNAs) are a class of small, noncoding RNAs of ~21–23 nucleotides that regulate gene expression at the posttranscriptional level (Ambros, 2001; Hobert, 2008). They mostly destabilize target mRNAs or suppress their translation by binding to complementary sequences in the 3′ untranslated region (3′UTR) (Filipowicz et al., 2008). However, miRNAs also target 5′UTRs or coding regions and, in a few cases, upregulate expression of their target mRNAs (Tay et al., 2008; Vasudevan et al., 2007). Many miRNAs are developmentally regulated and expressed in tissue-specific patterns, indicating important functions in development (Bushati and Cohen, 2007; Zhao and Srivastava, 2007). Despite rapid progress in understanding their functions, the precise roles of many miRNAs in the proliferation, migration, and differentiation of hESCs and hESC-derived hNPCs remain unknown.

Several miRNAs have been implicated in neuronal development in model organisms (Kosik, 2006; Gao, 2008). One, miR-9, is 100% conserved at the nucleotide sequence level from flies to humans, but its expression patterns and developmental functions are not conserved across species. In *Drosophila*, miR-9a is expressed in epidermal cells in developing embryos and in wing discs, where it ensures the precise specification of sensory organ precursors (SOPs) by down-regulating Senseless in non-SOP cells and also affects wing development through dLMO (Li et al., 2006; Biryukova et al, 2009). In zebrafish, miR-9 is expressed in the developing brain (e.g., in regions adjacent to the midbrain-hindbrain boundary) and promotes neurogenesis by suppressing Her5 and Her9 (Leucht et al., 2008). In rodents, miR-9 is specifically expressed in the brain and is abundant in neurogenic regions in embryos and adults (Deo et al., 2006). It has been implicated in embryonic Cajal-Retzius cell differentiation (Shibata et al., 2008), regulation of BK channel mRNA splice variants in response to alcohol (Pietrzykowski et al., 2008), and adult neural progenitor differentiation (Zhao et al., 2009). However, the exact functions of miR-9 in hNPCs are unknown. The mRNA targets of a specific miRNA can shift rapidly through evolution, and there are many more miRNAs in humans than in rodents (Ambros and Chen, 2007; Bartel, 2009). Moreover, miRNAs are potential molecular targets of therapeutic approaches. Thus, it is vital to understand the unique functions and targets of each miRNA in human cells.

Here we demonstrate a novel essential role for miR-9 in coordinating the proliferation and migration of hESCs-derived hNPCs at their early stage of maturation. We also identify the mRNA encoding stathmin, a protein that increases microtubule instability, as a novel key target of miR-9 to mediate its effects in these biological processes. Moreover, hNPCs without miR-9 showed enhanced migration when transplanted into the embryonic mouse brain or the adult brain of a mouse model of stroke. These studies identify a novel function for miR-9 in hNPCs.

NIH-PA Author Manuscript

NIH-PA Author Manuscript

NIH-PA Author Manuscript

Results

Neuronal Differentiation of hESCs

To differentiate H9 hESCs into postmitotic neurons, we combined two protocols (Li and Zheng, 2006; Zhang et al., 2001) with some modifications. This differentiation process includes neural induction, expansion of homogenous populations of hNPCs, and neuronal maturation (Figure 1A). Initial multilineage differentiation was induced by forming embryoid bodies (EBs), followed by neural induction and rosette formation in the presence of basic fibroblast growth factor 2 (FGF2) and serum-free N2 supplement for 12 days as described (Zhang et al., 2001). The appearance of elongated cells radially arranged in rosettes is the hallmark of neuroepithelial cells in the neural tube (Elkabetz et al., 2008). Rosette cells were isolated and expanded in suspension cultures for about 1 month to allow neurospheres to enlarge. After exposure to brain-derived neurotrophic factor (BDNF) and glial cell line–derived neurotrophic factor (GDNF), dissociated hNPCs from neurospheres differentiated into mostly postmitotic neurons that are immunopositive for the neuronal marker TUJ1 (Figure S1A).

In vitro neuronal differentiation of hESCs was monitored from the day cells were placed in suspension culture (0 DIV) to 60 DIV by immunocytochemistry and extensive mRNA expression profiling for neural markers. Relative gene expression analysis by quantitative RT-PCR (qRT-PCR) showed rapid loss of the pluripotent ESC markers NANOG and OCT4 (Figure 1B). The peak expression of the neural markers SOX2 and PAX6 (Figure 1B) upon rosette formation at 16 DIV indicated targeted differentiation to neural lineages, which was further confirmed by immunostaining for nestin and SOX2 (Figure S1C, D). Mechanically isolated rosette cells were then propagated in suspension culture to form neurospheres consisting of hNPCs. At this stage, most if not all the cells in neurospheres were immunopositive for nestin and SOX2 (Figure S1E, F), and only few cells expressed neuronal markers such as TUJ1 (Figure S1G). Terminal differentiation of the expanded progenitors (30–45 DIV) over 2 more weeks yielded a cell population (45–60 DIV) that contained more than 70% TUJ1-positive postmitotic neurons (Figure S1A). Accordingly, qRT-PCR showed a marked increase in the expression level of the neuronal marker MAP2 and no expression of the stem/progenitor cell markers SOX2 and PAX6 in terminally differentiated cells (Figure 1B). We also examined molecular markers (Elkabetz et al. 2008) that indicate different stages of maturation for hNPCs (Figure S1K-N). These analyses confirmed the differentiation of hESCs into hNPCs and postmitotic neurons.

MiR-9 Expression Starts at the Early Neurosphere Stage

Next we examined the expression of several miRNAs during neuronal differentiation of hESCs. miR-367, a marker of pluripotent ESCs (Suh et al., 2004), was highly expressed in hESCs and EBs, but its expression decreased significantly at later stages (Figure 1C). In contrast, miR-124, a miRNA found at high levels in postmitotic neurons (Logos-Quintana et al., 2002), was highly expressed in terminally differentiated human neuronal cultures (Figure 1C).

miR-9 expression was turned on at 16–20 DIV during neurosphere formation and increased in hNPCs before terminal differentiation (Figure 1C). In situ hybridization confirmed that miR-9 was not expressed in rosette cells but was highly expressed in neurospheres (Figure 1D-G). A scrambled probe (negative control) showed mere background staining at both stages (Figure 1H-K). MiR-9 was also expressed in MAP2-positive postmitotic human neurons (Figure 1L) and, at lower levels, in human astrocytes (Figure 1M).

Expression of miR-9*, which is processed from the opposite strand of the miR-9 precursor (pre-miR-9), mirrored that of miR-9 (Figure 1C). Pre-miR-9 is expressed from three

NIH-PA Author Manuscript

NIH-PA Author Manuscript

NIH-PA Author Manuscript

chromosomes in humans and rodents. Pre-miR-9-2 expression from chromosome 5 correlated with miR-9 expression at different stages of neural differentiation of hESCs (Figure 1C), while pre-miR-9-1 and pre-miR-9-3 were undetectable in hESC-derived hNPCs (data not shown), suggesting little or no expression.

miR-9 Promotes Early hNPC Proliferation

hNPCs undergo extensive proliferation during the early neurosphere stage. The temporally regulated expression of miR-9 in hNPCs at this stage raises the possibility that miR-9 may regulate expansion of the NPC pool. Studying loss-of-function phenotypes is a powerful way to elucidate the normal functions of endogenous miRNAs in particular developmental processes. To this end, we used a locked nucleic acid (LNA) antisense probe to knock down miR-9 activity in the early stage of hNPC maturation, when miR-9 just starts to be expressed. Since this probe shares considerable sequence similarity with miR-9*, we sought to ensure that the probe did not affect the interaction of miR-9* and its targets. We cotransfected HEK293 cells with anti-miR-9 and pre-miR-9-2 with artificial reporter constructs containing miR-9 or miR-9* binding sites in the 3′UTR. The anti-miR-9 LNA probe specifically inhibited miR-9 function but did not interfere with the interaction of miR-9* with its targets (Figure S2A).

Transfecting a high percentage of hNPCs in neurospheres is difficult. The best time for efficient transfection of dissociated neurospheres and to characterize targets of miR-9 in early hNPCs is the transition from rosettes to neurospheres at 16 DIV, shortly before miR-9 expression begins. Rosettes were extracted from surrounding cells with dispase at 16 DIV, mechanically dissociated into 10–50-cell aggregates, and divided into three suspension cultures for transfection. At 24 h after transfection with the anti-miR-9 LNA probe, the level of mature miR-9 in hESCs-derived neurospheres was markedly reduced and remained at that low level up to 96 h after transfection (Figure 2A). Even 6 days after anti-miR-9 LNA transfection, the level of miR-9 remained low (30–40%). Thus, all the experiments presented in this study examine the functions of endogenous miR-9 in newly formed hNPCs. Anti-miR-9 did not affect miR-9* expression in hNPCs (Figure 2B), indicating the specificity of the knockdown.

Neurospheres transfected with anti-miR-9 were morphologically similar to controls. Interestingly, loss of miR-9 activity reduced the size of neurospheres 5 days after the knockdown (Figure 2C); at 120 h, the mean diameter was 145 ± 7 ($n = 163$) versus 193 ± 11 μm in controls ($n = 134$) ($p < 0.001$) (Figure 2D). To confirm this finding in another established system of neural progenitor differentiation, we used rat primary cortical progenitor cells from E14.5 Sprague-Dawley rats (R&D Systems). MiR-9 was expressed in embryonic rat cortical NPCs and differentiating neurons and, to a lesser extent, primary astrocytes, as shown by qRT-PCR (Figure S2B). In contrast, miR-124 was highly expressed in postmitotic neurons derived from rat cortical NPCs (Figure S2C). Thus, rodent miR-9 expression in a rat primary culture system seems to mimic human miR-9 expression in hNPCs and their progeny. Loss of miR-9 also decreased the size of rat neurospheres (data not shown), as in hNPCs.

TUNEL analysis, performed to examine cell death, revealed that loss of miR-9 activity did not affect the survival of hNPCs in newly formed neurospheres (Figure 2E). We confirmed this result in embryonic rat NPCs (Figure S2D). Furthermore a lactate dehydrogenase assay showed no increased cytotoxicity after transfection of hNPCs with anti-miR-9 LNA probes (Figure 2F). Thus, miR-9 does not affect cell survival of NPCs, and the decreased size of human neurospheres after miR-9 knockdown does not likely result from increased apoptotic cell death.

NIH-PA Author Manuscript

NIH-PA Author Manuscript

NIH-PA Author Manuscript

To assess the proliferation rates of NPCs with or without miR-9 activity, we performed BrdU labeling experiments on hNPCs and rat cortical NPCs. Cell proliferation was markedly decreased when miR-9 activity was lost (Figure 2G). Cell counting analysis of dissociated embryonic rat cortical NPCs (monolayer culture) at different times after anti-miR-9 transfection showed slower proliferation in the absence of miR-9 (Figure S2E). To further confirm this finding, we used WST-1 cell proliferation reagent (Roche Applied Science), a water-soluble tetrazolium salt whose rate of cleavage by mitochondrial dehydrogenases correlates with the number of viable cells in culture. Knockdown of miR-9 slowed the proliferation of hNPCs (Figure 2H) and of rat cortical NPCs in monolayer culture or in suspension (Figure S2F, G). These findings strongly indicate that miR-9 is required to promote the proliferation of early human and embryonic rat NPCs.

To exclude the possibility that loss of miR-9 resulted in precocious differentiation of hNPCs, we performed the following experiments. Immunostaining of dissociated human neurospheres showed no effect of loss of miR-9 activity on neuronal differentiation. The cells kept their neural progenitor properties, as shown by expression of the progenitor marker nestin at 7 days after transfection of hNPCs (Figure 3A, D). Again, we used rat cortical NPCs and confirmed that loss of miR-9 activity did not lead to precocious differentiation of rat NPCs as indicated by the unchanged proportion of SOX2-, nestin-, TUJ1- or GFAP- positive rat cells (Figure S3). In a more detailed analysis of the expression of different molecular markers that are useful for following the sequential events controlling neural progenitor maturation and specification (Elkabetz et al., 2008), we confirmed that loss of miR-9 did not cause precocious differentiation and showed that it may even slow the maturation of hNPCs (Figure 3J). Three days after transfection of anti-miR-9 LNA probe, the levels of the neural progenitor cell markers PAX6 and SOX2 were increased, while the neurogenic transcription factor MEF2C was decreased in absence of miR-9. PAX6 and SOX2 were more highly expressed in the pluripotent rosette cells at 16 DIV than in neurospheres (Figure 1B). In contrast, MEF2C expression mimicked miR-9 expression during neuronal differentiation of hESCs (Figure S1N). Thus, these findings suggest that miR-9 loss of function delays progression of hNPCs to a more mature neural progenitor fate, indicating reduced proliferation in the absence of miR-9 activity is not due to their precocious differentiation.

MiR-9 Delays Early hNPC Migration In Vitro

Tight coordination of the proliferation, migration, and differentiation of NPCs is essential for the proper development of the nervous system (Ayala et al., 2007) and is equally important in the subventricular zone of the adult brain, where miR-9 is highly expressed (Deo et al., 2006). After knockdown of miR-9 in embryonic rat cortical NPCs, we noticed that many cells migrated radially out of the neurospheres, mainly in chains, onto the plastic substrate (Figure 4C, D). In contrast, 3 or 6 days after transfection of rat cortical NPCs with scrambled probe, the neurospheres remained largely intact, with many fewer cells migrating (Figure 4A, B). We quantified this migration phenotype in two ways. We measured the distance from the neurosphere to the nucleus of the most distant cell at various times after transfection (Figure 4E). Secondly, we counted the number of cells that migrated (Figure 4F). Quantitative analysis of both parameters from a large number of neurospheres demonstrated an essential role of miR-9 in limiting these cells migrating away from neurospheres (Figure 4E and F).

Next, we determined whether miR-9 also limits the migration of hESC-derived hNPCs at the early neurosphere stage, when miR-9 expression begins. Since hNPCs are difficult to culture and their migratory behavior has not yet been described, we tested several migration assays and culture conditions. The three-dimensional (3D) Matrigel cell migration assay proved most suitable (Gadea et al., 2007). Increasing evidence indicates that cellular behavior in a

NIH-PA Author Manuscript

NIH-PA Author Manuscript

NIH-PA Author Manuscript

3D environment reflects more accurately the in vivo situation. Neurospheres newly derived from hESCs were embedded in Matrigel/medium gel (1:1) 3 days after transfection with scrambled control or anti-miR-9, and cell migration was monitored (Figure 4G–L). Within 2.5 h, filamentous processes were seen outside neurospheres in which miR-9 activity was inhibited (Figure 4J) but not in controls (Figure 4G). Over the first 24 h, cells migrated from the neurospheres into the matrix, in chains or as individual cells. Both the number of cells that migrated and the distance from the edge of the neurospheres to the nucleus of the most distant migrating cells were significantly greater at 24 and 48 h after embedding in Matrigel (Figure 4M), at 4 and 5 days after transfection with anti-miR-9 and at later times (data not shown).

To further demonstrate that the migratory phenotype did not reflect precocious differentiation and that the cells maintained their neural progenitor properties, we stained cells for markers of NPCs and differentiated neurons or astrocytes 3 days after plating on Matrigel (6 days after transfection). Almost all migratory cells showed robust staining with the nestin antibody, with very few positive for TUJ1 or GFAP (Figure S4). Thus, migratory cells from the neurospheres at this early maturation stage maintained their neural progenitor properties without miR-9 activity. Furthermore, as shown in Figure 3, loss of miR-9 function in the early-hNPCs delayed their maturation process, which further supports our conclusion that miR-9 promotes proliferation and prevents excessive migration of early stage hNPCs.

MiR-9 Delays Early hNPC Migration In Vivo

To examine whether loss of miR-9 activity also affects the migratory behavior of hNPCs in vivo, we transfected neurospheres newly derived from hESCs with scrambled or anti-miR-9 LNA probes and transduced them with GFP-FUGW at 16 DIV. Two days after transfection, individual neurospheres with similar diameters were transplanted into the medial ganglionic eminence (MGE) of brain slices from E14.5 C57Bl/6 mouse embryos (Figure 5A). Four to five days later, many migrating cells maintained their progenitor identity, as shown by positive immunostaining for the progenitor marker nestin and negative staining for the postmitotic neuronal marker TUJ1 (Figure S5A-I). We measured the average of the five longest migrations of individual hNPCs in each brain slice. In the absence of miR-9 activity, more hNPCs migrated out from the neurospheres toward the neocortex and migrated 2.8-fold farther than control neurospheres (350 ± 26 μm (n = 34) versus 124 ± 22 μm, n = 29) (Figure 5B–D).

Migration of NPCs is important during development of the embryonic nervous system and also for repair after injury in the adult brain. To explore whether miR-9 can modulate the migration of transplanted hNPCs toward an injury site in the adult brain, we transfected hNPCs at 16 DIV with anti-miR-9 or control LNA probes. Neurospheres were dissociated 48 h later, and hNPCs (3×10^4) were transplanted into the striatum of immunodeficient adult mice 1 week after induction of permanent focal ischemia (Fig 5E), as described (Zhu et al., 2008). Migration was assessed 48 h after transplantation by immunostaining with an antibody against human mitochondria (hMit) and counting hMit-positive cells in four areas: 0–200, 200–400, 400–600, and > 600 μm away from the transplantation site (n = 8 mice per group). Control hNPCs were mostly confined to the bolus with limited radial migration (Figure 5F), but more hNPCs without miR-9 activity migrated toward the ischemic areas (Figure 5G, H). For instance, no control hNPCs were found beyond 400 μm. However, anti-miR-9 treated hNPCs were seen in the 400–600 μm area in seven of eight mice transplanted and beyond 600 μm in five (Figure 5H). The migrating hNPCs maintained their neural progenitor properties. For instance, migrating hNPCs labeled with hMit antibody did not express TUJ1 (Figure S5J-O).

NIH-PA Author Manuscript

NIH-PA Author Manuscript

NIH-PA Author Manuscript

Further analysis revealed that miR-9 knockdown increased the innate migratory potency of hNPCs in vivo. Although migration away from the ischemic area was observed (Figure S6E), more cells migrated toward the ischemic area than in the opposite direction, indicating a response to chemoattractants secreted from the ischemic brain region (Figure S6C, D, F). These results demonstrate a cell-autonomous function for miR-9 and enhanced in vivo migration of early hNPCs without miR-9 activity.

MiR-9 Regulates *Stathmin* Expression In Early hNPCs

To understand the mechanism by which miR-9 limits the migration of hESC-derived hNPCs, we searched for direct targets of miR-9 whose expression is downregulated at the onset of miR-9 expression. Using miRNA target prediction algorithms, including an unpublished one that considers both complementarity and target site accessibility (Fish et al., 2008), we identified several potential targets (Tables S1–S3). Most miRNAs decrease the stability of target mRNAs by cleavage or deadenylation (Filipowicz et al., 2008). Therefore, we used qRT-PCR to profile the expression of predicted target mRNAs at different stages of neural differentiation of hESCs. We then selected genes whose expression profiles negatively correlated with miR-9 expression during the early stage of hNPC maturation (16–20 DIV) (Table S4), including *STMN1* (stathmin), *CHMP2B* and *SIRT1* (Figure 6A).

To demonstrate whether the predicted targets are directly regulated by miR-9 at 16–20 DIV, we quantified mRNA expression by qRT-PCR in hNPCs 24 h after transfection with anti-miR-9. The mRNA and protein levels of stathmin, CHMP2B, and SIRT1 were significantly upregulated (Figure 6B, C). Moreover, overexpression of the miR-9 precursor (pre-miR-9-2) in HEK293 cells showed that stathmin, CHMP2B, and SIRT1 mRNA levels were reciprocally regulated by miR-9 abundance. Their expression was unchanged when the control miRNA, miR-124, was overexpressed (Figure 6D). Thus, these mRNAs are indeed regulated by miR-9 at the early neurosphere stage.

miR-9 regulates different targets in different model organisms (e.g. Li et al., 2006; Leucht et al., 2008; Pietrzykowski et al., 2008). Among its targets in hNPCs at the early neurosphere stage, the stathmin gene is most interesting. It encodes a developmentally regulated cytosolic phosphoprotein with a catastrophe-promoting microtubule-depolymerization activity (Belmont and Mitchison, 1996) and is prominently expressed in neuroproliferative zones of the brain and neuronal migratory pathways (Jin et al., 2004; Giampietro et al., 2005). Stathmin also regulates cell proliferation and promotes the motility of immortalized neuronal cells and human sarcoma cells (Giampietro et al., 2005; Rubin et al., 2004; Baldassarre et al., 2005). Thus, it may be a molecular link between miR-9 and hNPC migration. Stathmin mRNA has a predicted miR-9 binding site in the 3′UTR (Figure 6E), which is highly conserved from rodents to humans (Figure 6F).

To further demonstrate a direct interaction between miR-9 and stathmin mRNA, we cotransfected HEK293 cells with pre-miR-9-2 and a luciferase construct containing the 3′UTR of stathmin mRNA. We also generated a mutant 3′UTR in which three nucleotides in the seed region were altered to disrupt its interaction with miR-9 (Figure 6E). In luciferase assays, miR-9 suppressed stathmin expression directly through its interaction with the 3′UTR (Figure 6G). The effect of miR-9 on the reporter gene expression was lower than that on endogenous stathmin mRNA, probably because expression of the reporter gene was under the control of a strong promoter and transiently overexpressed. Thus, the molecular ratio of miR-target was different in the two experiments.

Moreover, the miR-9-stathmin interaction was abolished by transfecting a morpholino antisense oligonucleotide complementary to the 3′UTR of stathmin. This target protector

NIH-PA Author Manuscript

NIH-PA Author Manuscript

NIH-PA Author Manuscript

prevented mir-9 binding and reduced stathmin expression in HEK293 cells overexpressing miR-9 (data not shown). Thus, stathmin mRNA is a direct target of miR-9 in hNPCs.

Stathmin Mediates the Effects of MiR-9 in Early hNPCs

During neural differentiation of hESCs, stathmin is markedly downregulated only during the early neurosphere stage (16–20 DIV) (Figure 6A). To determine whether the miR-9/stathmin mRNA interaction modulates cellular behavior at this early stage of NPC maturation, we performed an epistasis experiment. Transfection of stathmin siRNA in hNPCs reduced the mRNA level by 76% (Figure S7A). The migration of the cells was not altered, but the effect of miR-9 knockdown on stathmin expression was significantly suppressed (Figure S7A) and the migratory phenotype of young hNPCs in the 3D Matrigel migration assay was rescued (Figure 7A–C). Moreover, loss of miR-9 activity promoted migration of rat NPCs away from neurospheres in a two-dimensional migration assay (Figure 7D–F). This phenotype, measured by the number of cells that migrated (Figure 7H) and the distance traveled (Figure 7G, I), was suppressed by simultaneous partial knockdown of stathmin. These findings indicate that stathmin is a key downstream target whose upregulation mediates the effect of loss of miR-9 on the migratory behavior of hNPCs.

Partial inhibition of stathmin by siRNA blocked the effect of loss of miR-9 on the proliferation of hNPCs in the WST-1 assay (Figure 7J) and also increased the proliferation of rat cortical NPCS in monolayer or in suspension cultures (Figure S7B and C). More importantly, we used two different siRNA constructs to partially inhibit stathmin expression in anti-miR-9 LNA-treated hNPCs and then transplanted these cells into the medial ganglionic eminence of brain slices from E14.5 C57Bl/6 mouse embryos. The enhanced migration of hNPCs in the absence of miR-9 activity in this in vivo environment was also suppressed by reduced stathmin activity (Figure 7K). These findings demonstrate that stathmin is a key target essential for miR-9 to coordinate the proliferation and migration of hNPCs in vitro and in vivo (Figure S7D).

Discussion

Stem cell–based transplantation therapies for brain injuries and degenerative diseases hold great promise but also face major challenges, including the risk of uncontrolled proliferation and tumor formation and the failure to migrate to injured brain regions and properly incorporate into the damaged neuronal circuitry. Our findings here demonstrate an unexpected role for miR-9 in coordinating the proliferation and migration of young hNPCs derived from hESCs. Loss of miR-9 activity enhanced the migration of hNPCs transplanted into embryonic or adult mouse brains in a stroke model. Since so little is known about the cellular behavior of human neurons and their progenitor cells, our results may help improve the clinical efficacy of cell therapies in the nervous system using hESCs or iPS cells.

There are at least 400 miRNAs in humans and many of them are not evolutionarily conserved, suggesting human-specific functions. However, few have been studied with loss-of-function approaches (Bartel, 2009). hESCs are an excellent model system for studying the physiological functions and specific targets of each endogenous human miRNA in different human cell types, such as in neural progenitors during neuronal specification from hESCs. To this end, the loss-of-function studies are critically important. Such approaches have been widely used in other model organisms. For instance, genetic knockout of miR-9 in *Drosophila* revealed an essential role in ensuring the precision of SOP specification (Li et al., 2006). Morpholino knockdown in zebrafish indicated a role for miR-9 in regulating the organizing activity and neurogenesis at the midbrain-hindbrain boundary (Leucht et al., 2008). Interestingly, although miR-9 is 100% conserved at the sequence level, its expression patterns and functions differ significantly in different organisms (Delaloy and Gao, 2008). In

NIH-PA Author Manuscript

NIH-PA Author Manuscript

NIH-PA Author Manuscript

neuronal differentiation of hESCs, miR-9 expression is specifically turned on in hNPCs and maintained in postmitotic neurons. Our cell transplantation experiments further demonstrate a novel cell-autonomous function for miR-9 in regulating the migratory behavior of hNPCs.

Each miRNA may regulate hundreds of target mRNAs (Bartel, 2009). It is possible many miRNAs exert their functions in a specific biological process mainly through a few target mRNAs. For instance, Senseless seems to be the key target in miR-9a regulation of SOP specification in *Drosophila* (Li et al., 2006). At the midbrain-hindbrain boundary in zebrafish, several components of the FGF signaling pathway is targeted by miR-9 (Leucht et al., 2008). In fly wing development, dLMO is another key target of miR-9a (Biryukova et al., 2009). It was reported that miR-9 suppressed the expression of the transcription factor Foxg1 but not the nuclear receptor Tlx (also known as Nr2e1) during Cajal-Retzius cell differentiation (Shibata et al., 2008). However, another report suggested that overexpression of miR-9 suppressed the expression of Tlx during the terminal differentiation of adult mouse neural progenitor cells, resulting in increased differentiation and migration of newborn neurons (Zhao et al., 2009). The reasons for this discrepancy are unknown. In our current study, stathmin seems to be a novel key target that is essential for miR-9 to promote proliferation and limit migration of multipotent hNPCs in the early neurosphere stage. Thus, this specific miR–target interaction is essential to maintain the hNPC pool at this particular stage. This conclusion, based on extensive loss-of-function studies both in cell culture and in transplantation experiments in mouse brains, does not exclude the likely possibility that some other miR-9 targets are also essential in this process.

There are several significant differences between the study by Zhao et al. and ours. First, we used hESC-derived neural progenitors instead of adult mouse neural progenitors. Second, we performed our studies using loss-of-function approaches to examine the physiologically relevant functions of endogenous miR-9 in newly formed hNPCs. After miR-9 knockdown, hESC-derived hNPCs maintained their neural progenitor properties and exhibited enhanced migration, both in vitro and after transplantation into mouse embryonic or adult brains. In contrast, Zhao et al. reported that migrating cells after miR-9 overexpression expressed neuronal but not progenitor markers, and they failed to detect a change in cell differentiation in NPCs treated with miR-9 antisense RNA. Third, the miR-9–*Tlx* mRNA interaction was thought to be relevant only in adult neural progenitors shortly before terminal differentiation was induced with retinoic acid or forskolin (Zhao et al., 2009). In contrast, we studied newly formed hNPCs before the expansion of the progenitor pool. Thus, the same miRNA may have distinct functions at different developmental stages of various NPCs, likely by regulating different spatially and temporally expressed mRNA targets (Figure S7D).

The molecular interaction between miR-9 and stathmin may have important implications for other biological processes as well. For instance, miR-9 is overexpressed in primary but not metastatic brain tumors (Nass et al., 2008), and stathmin enhances cancer cell migration and the metastatic phenotype (Baldassarre et al., 2005; Rosenfeld et al., 2008). Thus, manipulation of the miR-9–stathmin interaction may suppress tumor formation and enhance the migration of transplanted hNPCs and is therefore a potential target for improving the efficacy of stem cell–based therapies.

Experimental Procedures

Neural Differentiation of hESCs

Human ES cells (H9, passages 30–45; WiCell Research Institute) were cultured on a layer of mouse embryonic fibroblasts (MEFs) (PMEF-CFL, Chemicon), previously inactivated with mitomycin C (Roche), in DMEM/F12 medium supplemented with 20% knockout serum replacement, 1 mM L-glutamine, 1% nonessential amino acids, and 4 ng/ml human FGF2

NIH-PA Author Manuscript

NIH-PA Author Manuscript

NIH-PA Author Manuscript

(Invitrogen) and 0.1 mM 2-mercaptoethanol (Chemicon). The medium was changed daily, and cells were passaged every 4–6 days with 1 mg/ml collagen IV (Invitrogen). Neural differentiation was induced as described with some modifications (Li and Zheng, 2006; Zhang et al., 2001). Details can be found in supplemental information.

Primary Culture of Rat Embryonic Cortical Neural Progenitor Cells (NPCs)

Rat embryonic cortical NPCs (R&D Systems) were cultured as a monolayer in StemXVivo serum-free NSC Base medium, according to the manufacturer's protocol (R&D Systems) supplemented with 20 ng/ml human FGF2 (Invitrogen) on plates coated with poly-L-ornithine- and fibronectine (Sigma). Fresh FGF2 was added each day, and the medium was replaced every 2 days. Only passages 1–3 were used for experiments. The neurosphere culture system was used according to the manufacturer's protocol (R&D Systems).

Analysis of miRNA and mRNA Expression

Total RNA was extracted and purified with the miRNeasy kit (Quiagen) and the Turbo DNA free kit (Ambion). miRNA expression levels were quantified with TaqMan microRNA assays (Applied Biosystems). Endogenous controls used for real-time quantification are described in the supplemental information.

Real-time PCR analyses were performed in duplicate in 20-μl volumes for at least three independent cultures. mRNA expression analysis is described in the supplemental information.

Knockdown of MiR-9 and STMN1

hNPCs at 16 DIV and rat cortical NPCs were transiently transfected with miRCURY LNA knockdown probes (Exiqon) with Lipofectamine 2000 (Invitrogen) after additional mechanical dissociation into small clumps (10–50 cells). A scrambled miRNA, 5′-gtgtaacacgtctatacgccca, which bears no homology to any known miRNA or mRNA sequences in human, mouse, and rat, was used as negative control, and hsa-anti-miR-9 (100 nM) was used to specifically inhibit miR-9. Stathmin was knocked down with Silencer Select pre-designed siRNA (s8091 and s8093 at 20 nM; Ambion); Silencer Select Negative Control 1 siRNA (Ambion) was used as negative control.

3′UTR Reporter Assays

The full-length (447 bp) 3′UTR of the human stathmin gene and a fragment (100 bp) containing the putative miR-9 binding site were amplified from human genomic DNA and individually cloned into the pGl3-promoter vector (Promega). A mutant construct with three base changes (CAA to GTT) in the seed region of the miR-9 binding site was also generated. Pre-miR-9-2 was amplified from a bacterial artificial chromosome containing the mouse genomic *miR-9-2* sequence (bMQ-381K3; GeneService) and cloned into the pSUPER vector under the control of the H1 promoter (OligoEngine). Transient transfection of HEK 293 cells and gene reporter assays were carried out as described (Li et al. 2006).

In Situ Hybridization and Immunostaining

5′-Fluorescein-labeled miR-9 miRCURY detection probe (Exiqon) was used to detect miR-9 expression in neurospheres. After immunostaining and fixation, the cells were subjected to in situ hybridization as described (Politz et al., 2006). For immunocytochemistry, cells were fixed with 4% paraformaldehyde (PFA) for 10 min at room temperature and incubated with primary antibody overnight at 4°C. Staining with secondary antibodies was performed for 1 h at room temperature followed by Hoechst staining.

NIH-PA Author Manuscript

NIH-PA Author Manuscript

NIH-PA Author Manuscript

Cell Proliferation and Viability Assays

TUNEL assay—The i*n situ* cell death detection kit TMR Red (Roche) was used to label apoptotic cells according to the manufacturer's instructions. Neurospheres were attached on Matrigel-coated flasks for a few hours before TUNEL assay to allow better pictures of the cells.

Cytotoxicity Analysis—To assess the cytotoxicity of anti-miR-9 LNA, we measured LDH released into culture medium upon cell lysis, using a nonradioactive cytotoxicity assay kit (CytoTox 96, Promega). See supplemental information for details.

BrdU Staining—Neurospheres were attached on Matrigel-coated flasks for a few hours before BrdU staining to allow better pictures of the cells. BrdU (10 μM) was added to the culture medium for 4 h. Cells were fixed in 4% paraformaldehyde and stained with anti-BrdU antibodies (Abcam) according the manufacturer's instructions. Cells were stained with Hoechst to quantify the proportion of BrdU-positive cells in several random fields. Over 500 cells were counted in each experiment, and the experiments were performed in triplicate.

WST1 proliferation assay—Proliferating cells were detected at various times with the WST1 cell-proliferation assay (Roche Applied Science), and cell proliferation was measured according to the manufacturer's instructions. hES-derived neurospheres were transfected with control or anti-miR-9 at 16 DIV. The next day, they were seeded in 96-well plates (8 to16 wells per conditions and time point). The average absorbance at 450 nm for each time point was normalized to the value on day 1 after transfection.

In Vitro Migration Assays

All migration experiments with rat cortical NPCs were performed in the presence of FGF2 and epidermal growth factor on plastic substrates. One day after transfection with Lipofectamine 2000, half of the medium was replaced with fresh medium. Culture dishes were handled carefully to keep the neurospheres at the bottom. Cell migration was evaluated by counting cells that had migrated out from the neurospheres and measuring the distance from the edge of the neurosphere to the nucleus of the most distant cell.

hNPCs were analyzed in a three-dimensional cell migration assay. Matrigel (BD Biosciences) was diluted by half in neural induction medium, and 70 μl of the mix was dispensed per well in a 96-well plate and allowed to polymerize at 37°C overnight. Neurospheres (3 days after transfection) were placed onto the polymerized Matrigel matrix and covered with 70 μl of Matrigel.

In Vivo Migration Assays

Neurospheres ~150 μm in diameter were transplanted into the medial ganglionic eminence, of coronal forebrain slices (see supplemental informations for details) using a glass pipette 150 μm in diameter to control for the size of the neurospheres (Wichterle et al., 1999). The cocultures were maintained in DMEM/F12 medium supplemented with 10% fetal calf serum and high glucose. Four days after transplantation, hNPCs were visualized by fluorescence microscopy, and the distance between the migratory cells and the edge of the transplanted neurospheres was measured. The migration of transplanted hNPCs in mouse brain slices was quantified in terms of the maximum distance described in the supplemental information.

Permanent focal ischemia was induced in eight adult male CD-1 nude mice (Charles River Laboratories) in each experiment by distal middle cerebral artery occlusion. One week later, hNPCs transfected with scrambled or anti-miR-9 LNA probes (1×10^4 cells/μl) were injected at a rate of 0.2 μl/min into the striatum of each randomly picked mouse. Mice were

NIH-PA Author Manuscript

NIH-PA Author Manuscript

NIH-PA Author Manuscript

sacrificed 48 h later, and 30-μm-thick frozen coronal brain sections were immunostained with the anti-human mitochondria antibody (1:40, Chemicon). Most cells migrated toward the injury site. We divided the migratory path into four sampling areas, 0-200, 200–400, 400–600 μm, and >600 μm away from the transplanted hNPCs. Using ImageJ software, we counted hMit-positive migrating cells and determined the percentages of cells in each area. In each mouse, the average from two to three coronal slices was obtained. Eight brains from two independent experiments were analyzed for each condition.

Western Blotting

SDS-PAGE and western blotting were performed according to standard procedures. b-Actin on the same membrane served as the loading control. The primary antibodies used were anti-CHMP2B (Abcam AB33174), anti-stathmin (Cell Signaling Technology), and anti-SIRT1 (gift of E. Verdin). Densitometry analysis was carried out in Photoshop. The relative intensity is the average of three different experiments.

Supplementary Material

Refer to Web version on PubMed Central for supplementary material.

Acknowledgments

We thank J. Rubenstein, D. Srivastava, and our lab members for discussions and comments, G. Howard and S. Ordway for editorial assistance, and S. Mitchell for administrative assistance. C.D. would like to thank Bettencourt Schueller Foundation for help with relocation to San Francisco. C.D. and J.-A.L. are supported by fellowships from the California Institute for Regenerative Medicine (CIRM). This work is supported by grants from the CIRM (F.-B.G.) and the NIH (F.-B.G. and W.L.Y.).

References

Ambros V. microRNAs: tiny regulators with great potential. Cell 2001;107:823–826. [PubMed: 11779458]

Ambros V, Chen X. The regulation of genes and genomes by small RNAs. Development 2007;134:1635–1641. [PubMed: 17409118]

Ayala R, Shu T, Tsai LH. Trekking across the brain: the journey of neuronal migration. Cell 2007;128:29–43. [PubMed: 17218253]

Baldassarre G, et al. p27(Kip1)-stathmin interaction influences sarcoma cell migration and invasion. Cancer Cell 2005;7:51–63. [PubMed: 15652749]

Bartel DP. MicroRNAs: Target recognition and regulatory functions. Cell 2009;136:215–233. [PubMed: 19167326]

Belmont LD, Mitchison TJ. Identification of a protein that interacts with tubulin dimers and increases the catastrophe rate of microtubules. Cell 1996;84:623–631. [PubMed: 8598048]

Biryukova I, Asmar J, Abdesselem H, Heitzler P. Drosophila mir-9a regulates wing development via fine-tuning expression of the LIM only factor, dLMO. Dev Biol 2009;327:487–496. [PubMed: 19162004]

Bushati N, Cohen SM. microRNA functions. Annu Rev Cell Dev Biol 2007;23:175–205. [PubMed: 17506695]

Cobos I, Borello U, Rubenstein JL. Dlx transcription factors promote migration through repression of axon and dendrite growth. Neuron 2007;54:873–888. [PubMed: 17582329]

Delaloy C, Gao FB. MicroRNA-9 multitasking near organizing centers. Nat Neurosci 2008;11:625–626. [PubMed: 18506136]

Deo M, Yu JY, Chung KH, Tippens M, Turner DL. Detection of mammalian microRNA expression by in situ hybridization with RNA oligonucleotides. Dev Dyn 2006;235:2538–2548. [PubMed: 16736490]

NIH-PA Author Manuscript NIH-PA Author Manuscript NIH-PA Author Manuscript

Duan X, Kang E, Liu CY, Ming GL, Song H. Development of neural stem cell in the adult brain. Curr Opin Neurobiol 2008;18:108–115. [PubMed: 18514504]

Elkabetz Y, et al. Human ES cell-derived neural rosettes reveal a functionally distinct early neural stem cell stage. Genes Dev 2008;22:152–165. [PubMed: 18198334]

Filipowicz W, Bhattacharyya SN, Sonenberg N. Mechanisms of posttranscriptional regulation by microRNAs: Are the answers in sight? Nat Rev Genet 2008;9:102–114. [PubMed: 18197166]

Fish JE, et al. miR-126 regulates angiogenic signaling and vascular integrity. Dev Cell 2008;15:272–284. [PubMed: 18694566]

Gadea G, de Toledo M, Anguille C, Roux P. Loss of p53 promotes RhoA-ROCK-dependent cell migration and invasion in 3D matrices. J Cell Biol 2007;178:23–30. [PubMed: 17606864]

Gao FB. Posttranscriptional control of neuronal development by microRNA networks. Trends Neurosci 2008;31:20–26. [PubMed: 18054394]

Giampietro C, et al. Stathmin expression modulates migratory properties of GN-11 neurons in vitro. Endocrinology 2005;146:1825–1834. [PubMed: 15625246]

Hobert O. Gene regulation by transcription factors and microRNAs. Science 2008;319:1785–1786. [PubMed: 18369135]

Hochedlinger K, Jaenisch R. Nuclear transplantation, embryonic stem cells, and the potential for cell therapy. N Engl J Med 2003;349:275–286. [PubMed: 12867612]

Jin K, et al. Proteomic and immunochemical characterization of a role for stathmin in adult neurogenesis. FASEB J 2004;18:287–299. [PubMed: 14769823]

Kosik KS. The neuronal microRNA system. Nat Rev Neurosci 2006;7:911–920. [PubMed: 17115073]

Lagos-Quintana M, et al. Identification of tissue-specific microRNAs from mouse. Curr Biol 2002;30:735–739. [PubMed: 12007417]

Leucht C, et al. MicroRNA-9 directs late organizer activity of the midbrain-hindbrain boundary. Nat Neurosci 2008;11:641–648. [PubMed: 18454145]

Li XJ, Zheng SC. In vitro differentiation of neural precursors from human embryonic stem cells. Methods Mol Biol 2006;331:169–177. [PubMed: 16881517]

Li Y, Wang F, Lee JA, Gao FB. MicroRNA-9a ensures the precise specification of sensory organ precursors in Drosophila. Genes Dev 2006;20:2793–2805. [PubMed: 17015424]

Mao Y, Ge X, Frank CL, Madison JM, Koehler AN, Doud MK, Tassa C, Berry EM, Soda T, Singh KK, Biechele T, Petryshen TL, Moon RT, Haggarty SJ, Tsai LH. Disrupted in schizophrenia 1 regulates neuronal progenitor proliferation via modulation of GSK3beta/beta-catenin signaling. Cell 2009;136:1017–1031. [PubMed: 19303846]

Nass D, et al. MicroRNAs accurately identify cancer tissue origin. Nat Biotechnol 2008;26:462–469. [PubMed: 18362881]

Pietrzykowski AZ, Friesen RM, Martin GE, Puig SI, Nowak CL, Wynne PM, Siegelmann HT, Treistman SN. Posttranscriptional regulation of BK channel splice variant stability by miR-9 underlies neuroadaptation to alcohol. Neuron 2008;59:274–287. [PubMed: 18667155]

Politz JC, Zhang F, Pederson T. MicroRNA-206 colocalizes with ribosome-rich regions in both the nucleolus and cytoplasm of rat myogenic cells. Proc Natl Acad Sci U S A 2006;103:18957–18962. [PubMed: 17135348]

Rosenfeld N, et al. Stathmin activity influences sarcoma cell shape, motility, and metastatic potential. Mol Biol Cell 2008;19:2003–2013. [PubMed: 18305103]

Rubin CI, Atweh GF. The role of stathmin in the regulation of the cell cycle. J Cell Biochem 2004;93:242–250. [PubMed: 15368352]

Shibata M, Kurokawa D, Nakao H, Ohmura T, Aizawa S. MicroRNA-9 modulates Cajal-Retzius cell differentiation by suppressing Foxg1 expression in mouse medial pallium. J Neurosci 2008;28:10415–10421. [PubMed: 18842901]

Suh MR, et al. Human embryonic stem cells express a unique set of microRNAs. Dev Biol 2004;270:488–498. [PubMed: 15183728]

Tay Y, Zhang J, Thomson AM, Lim B, Rigoutsos I. MicroRNAs to Nanog, Oct4 and Sox2 coding regions modulate embryonic stem cell differentiation. Nature 2008;455:1124–1128. [PubMed: 18806776]

NIH-PA Author Manuscript

NIH-PA Author Manuscript

NIH-PA Author Manuscript

Vasudevan S, Tong Y, Steitz JA. Switching from repression to activation: microRNAs can up-regulate translation. Science 2007;318:1931–1934. [PubMed: 18048652]

Wichterle H, Garcia-Verdugo JM, Herrera DG, Arturo Alvarez-Buylla A. Young neurons from medial ganglionic eminence disperse in adult and embryonic brain. Nat Neurosci 1999;2:461–466. [PubMed: 10321251]

Yamanaka S. Strategies and new developments in the generation of patient-specific pluripotent stem cells. Cell Stem Cell 2007;7:39–49. [PubMed: 18371333]

Yu J, Thomson JA. Pluripotent stem cell lines. Genes Dev 2008;22:1987–1997. [PubMed: 18676805]

Zhang SC, Wernig M, Duncan ID, Brüstle O, Thomson JA. In vitro differentiation of transplantable neural precursors from human embryonic stem cells. Nat Biotechnol 2001;19:1129–1133. [PubMed: 11731781]

Zhao C, Deng W, Gage FH. Mechanisms and functional implications of adult neurogenesis. Cell 2008;132:645–660. [PubMed: 18295581]

Zhao C, Sun G, Li S, Shi Y. A feedback regulatory loop involving microRNA-9 and nuclear receptor TLX in neural stem cell fate determination. Nat Struct Mol Biol 2009;16:365–371. [PubMed: 19330006]

Zhao Y, Srivastava D. A developmental view of microRNA function. Trends Biochem Sci 2007;32:189–197. [PubMed: 17350266]

Zhu W, Fan Y, Frenzel T, Gasmi M, Bartus RT, Young WL, Yang GY, Chen Y. Insulin growth factor-1 gene transfer enhances neurovascular remodeling and improves long-term stroke outcome in mice. Stroke 2008;39:1254–1261. [PubMed: 18309153]

NIH-PA Author Manuscript

NIH-PA Author Manuscript

NIH-PA Author Manuscript

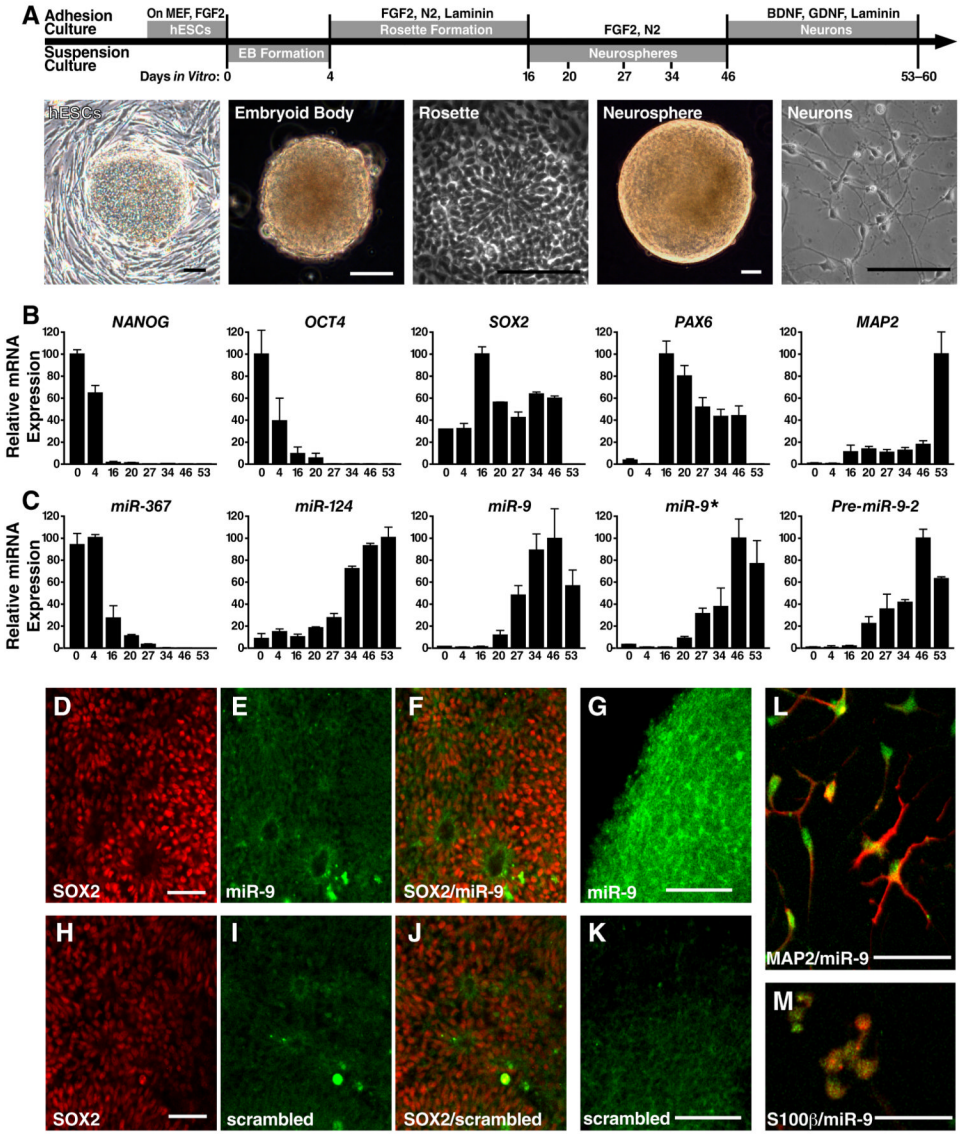

Figure 1. MiR-9 Expression During Neural Differentiation of hESCs

(A) Phase-contrast images of cells at different stages of neural differentiation of hESCs. hESCs (H9 line) were maintained in the presence of FGF2 on mouse embryonic fibroblast (MEF) feeder cells. DIV 0 is the day hESCs were dissociated from MEFs. Initial differentiation was induced by the formation of EBs, followed by neural induction in the presence of FGF2 and N2 supplements. Rosette-forming colonies of neuroectodermal cells appeared at 13–16 DIV. Neural progenitors in rosettes were dissociated and expanded in suspension cultures at 16–46 DIV to form neurospheres. Dissociated neural progenitors were exposed to BDNF and GDNF to differentiate into neurons at 43–60 DIV. Scale bar, 100 μm.

(B) Expression profiles of cellular markers monitored by qRT-PCR at different stages of neural differentiation. Values on *x*-axis are DIV after culturing hESCs in suspensions. Expression was normalized to GAPDH levels, and the highest level for a given marker was always taken as 100. Values are mean ± s.e.m. from at least three independent cultures. *NANOG* and *OCT4* are markers of pluoripotent ESCs. *SOX2* and *PAX6* are expressed in neural progenitors, and *MAP2* is a marker of mature neurons.

NIH-PA Author Manuscript

NIH-PA Author Manuscript

NIH-PA Author Manuscript

(C) Expression profiles of miR-367, an miRNA highly enriched in stem cells; miR-124, an miRNA highly enriched in postmitotic neurons; and miR-9, miR-9*, and pre-miR-9-2, which gives rise to miR-9 and miR-9* during neural differentiation of hESCs.

(D-M) In situ analysis of MiR-9 expression during hESC neural differentiation.

(D-F) miR-9 is not expressed in SOX2-positive rosette structures as shown by the lack of miR-9 in situ labeling in SOX2-immunopositive cells.

(G) miR-9 is strongly expressed in neurospheres as indicated by the green signal of in situ labeling.

(H-J) Scrambled control probe was used as a negative control to show the background in situ labeling in SOX2-positive cells in rosette structures.

(K) Scrambled control probe did not label hNPCs in neurospheres.

(L) miR-9 (as indicated in green) was expressed in MAP-2 positive human neurons (as indicated by red).

(M) miR-9 (as indicated in green) is also expressed at a low level in S100b-positive astrocytes (as indicated by red).

See also Figure S1.

NIH-PA Author Manuscript

NIH-PA Author Manuscript

NIH-PA Author Manuscript

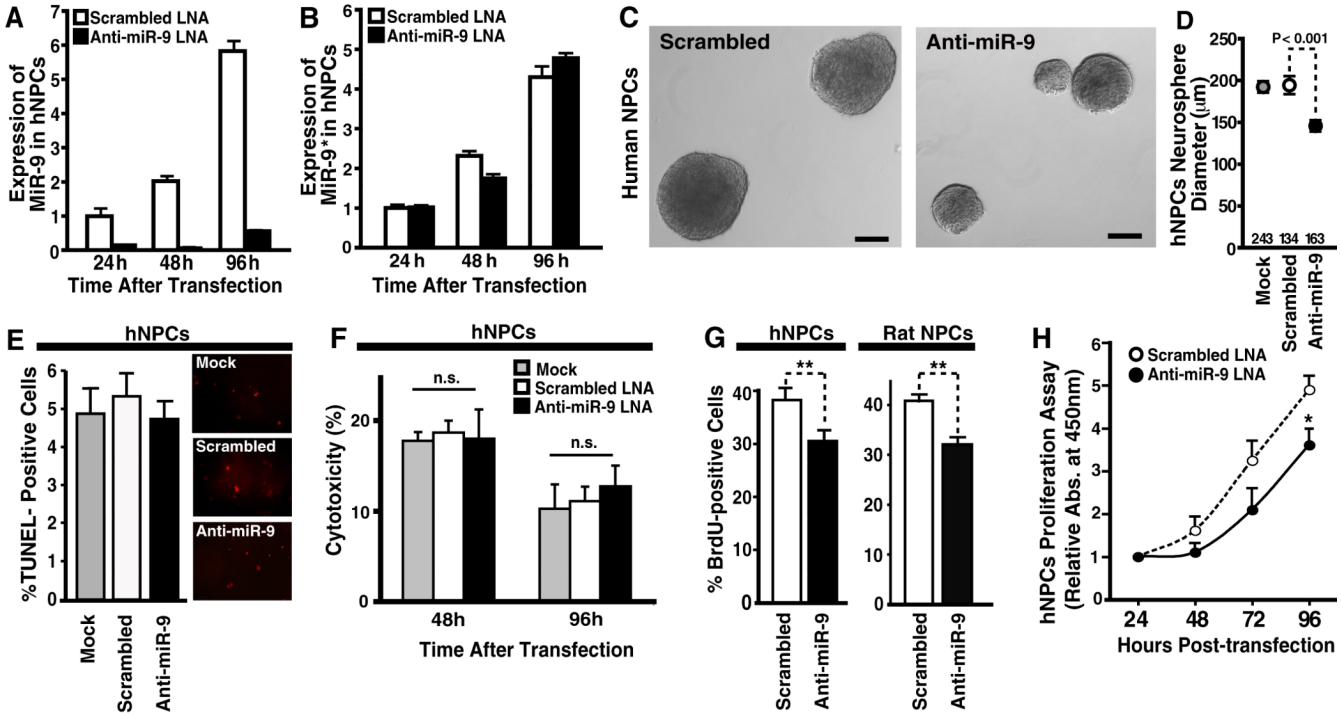

Figure 2. MiR-9 Is Required to Promote Proliferation of Early Neural Progenitors

(A, B) The LNA-anti-miR-9 probe complementary to miR-9 was introduced at 16 DIV in dissociated human NPCs dissected from rosettes and cultured in suspension. Relative levels of mature miR-9 (A) and miR-9* (B) were measured by qRT-PCR 24, 48, and 96 h after transfection with anti-miR-9 or control scrambled probe.

(C) Phase-contrast images of hESC-derived neurospheres transfected with scrambled or anti-miR-9 probe. Scale bar, 100 µm.

(D) Neurosphere diameters 5 days after transfection. Numbers on *x*-axis indicate the number of neurospheres measured. Values are mean ± s.e.m.

(E) TUNEL staining indicates that loss of miR-9 does not affect the survival of human neural progenitors. Quantification and representative images of TUNEL staining are presented.

(F) MiR-9 knockdown does not have a cytotoxic effect on hNPCs. hESC-derived neural progenitors were mock transfected or transfected with a scrambled LNA probe or with anti-miR-9 LNA probe at 16 DIV. Medium was changed 20 h before LDH assays for cytotoxicity 48 h and 96 h after transfection. n.s.: not significant. Values are mean ± s.e.m.

(G) BrdU incorporation was decreased in hNPCs and rat NPCs when miR-9 was knocked down. The percentage of BrdU-positive cells at 3 days after transfection is shown. Values are mean ± s.e.m. $^{**}P < 0.01$ ($n = 3$).

(H) hNPCs were transfected with the LNA-anti-miR-9 or scrambled probe at 16 DIV of neuronal differentiation. Neurospheres were collected 24 h later and split in 96-well plates. Metabolic activity was measured (Abs. 450 nm) using WST-1 proliferation assay at this time point and every day. The average absorbance for each time point was normalized to the value on day 1 after transfection. Values are mean ± s.e.m of 8 to 16 wells per time point and per conditions. $^{*}P < 0.05$.

See also Figure S2.

NIH-PA Author Manuscript

NIH-PA Author Manuscript

NIH-PA Author Manuscript

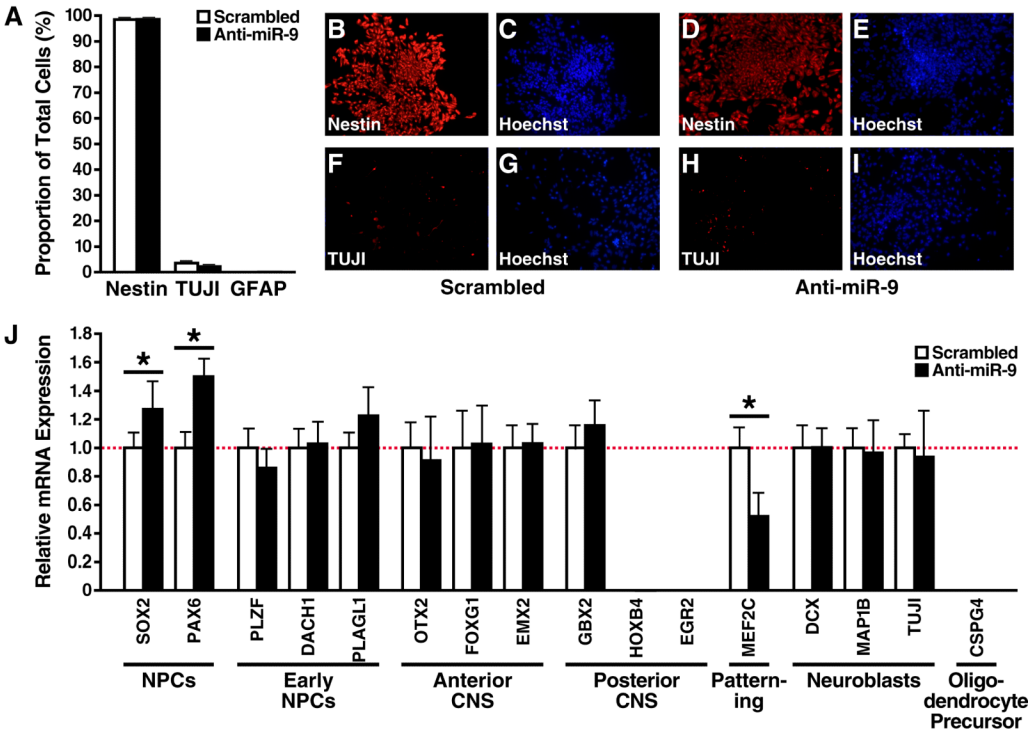

Figure 3. Loss of miR-9 Function Delays Early Neural Progenitor Maturation

(A-I) MiR-9 knock down does not lead to precocious differentiation of rat embryonic NPCs as shown by immunostaining.

(A) Proportions of cells expressing the given marker among all human cells at the neurosphere stage visualized by nuclear staining. No difference is observed between the scrambled and anti-miR-9 transfected cells 7 days after transfection of hNPCs.

(B-I) Expression of the neural progenitor marker nestin (B, D) and the neuronal marker TUJ1 (F, H) in control or anti-miR-9-transfected hNPCs. C, E, G, and I show nuclear staining in blue.

(J) qRT-PCR analysis of the expression levels of molecular markers for neural progenitors. Three days after transfection with scrambled or anti-miR-9 LNA probe, total RNAs were extracted from cells in the newly formed neurospheres and analyzed by qRT-PCR. Markers analyzed include those common to neural stem cells (PAX6, SOX2), specific to the early state of neural progenitors (PLAGL1, DACH1, PLZF), expressed in neuroblasts (TUJ1, DCX, NEUROD1, MAP1B), specific for the anterior (OTX2, EMX2, FOXG1) or the posterior (GBX2, HOXB4, EGR2) identity, oligodendrocyte precursor marker (CSPG4), and neurogenic factor (MEF2C). Three days after transfection of anti-miR-9 LNA probe, the levels of PAX6 and SOX2 were increased, while the level of MEF2C was decreased, indicating delayed maturation.

However, no switch toward an anteroposterior identity was observed, and the neuroblast markers were not affected by loss of miR-9 function. Indeed the expression levels of early-NPCs markers did not change when miR-9 is inhibited. Thus, loss of miR-9 activity did not cause premature differentiation of neural progenitors. In fact, it suggests the loss of function delayed progression of hNPCs to a more mature neuronal progenitor fate. Values are mean ± s.e.m. *P <0.05.

See also Figure S3.

NIH-PA Author Manuscript

NIH-PA Author Manuscript

NIH-PA Author Manuscript

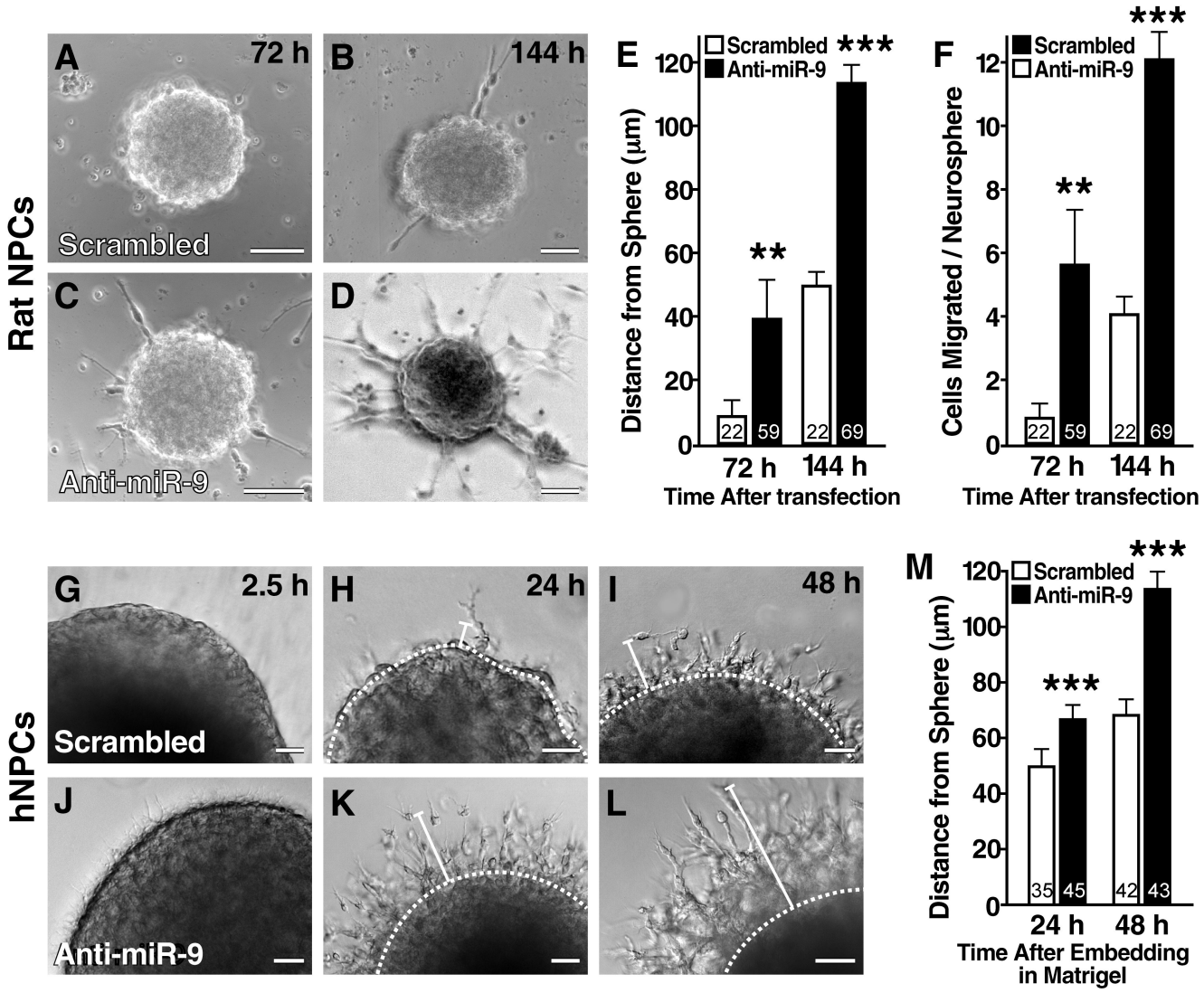

Figure 4. MiR-9 Limits Migration of hNPCs in Vitro

(A-D) miR-9 knockdown caused rat NPCs to migrate away from neurospheres on plastic substrate. The cells were cultured for 72 h and 144 h after transfection with scrambled control (A, B) or anti-miR-9 (C, D).

(E) Distance from the edge of the neurospheres to the most distant nucleus of the migrating cells. Values are mean ± s.e.m.

(F) Number of migrating cells with or without miR-9 activity. Values are mean ± s.e.m. In panels E and F, the number of neurospheres analyzed is indicated in each column.

(G-L) miR-9 knockdown resulted in precocious migration of hNPCs from the neurospheres cultured in the 3D matrix. hNPCs were dissociated from rosettes at 16 DIV, transfected, cultured for 3 days in suspension, and embedded in Matrigel; the time embedding is indicated.

(M) Distance from the edge of the neurosphere to the most distant nucleus of the outmigrating cells. Values are mean ± s.e.m. from 35 control and 45 miR-9-transfected neurospheres at 24 h and 42 control and 43 transfected neurospheres at 48 h.

See also Figure S4.

NIH-PA Author Manuscript

NIH-PA Author Manuscript

NIH-PA Author Manuscript

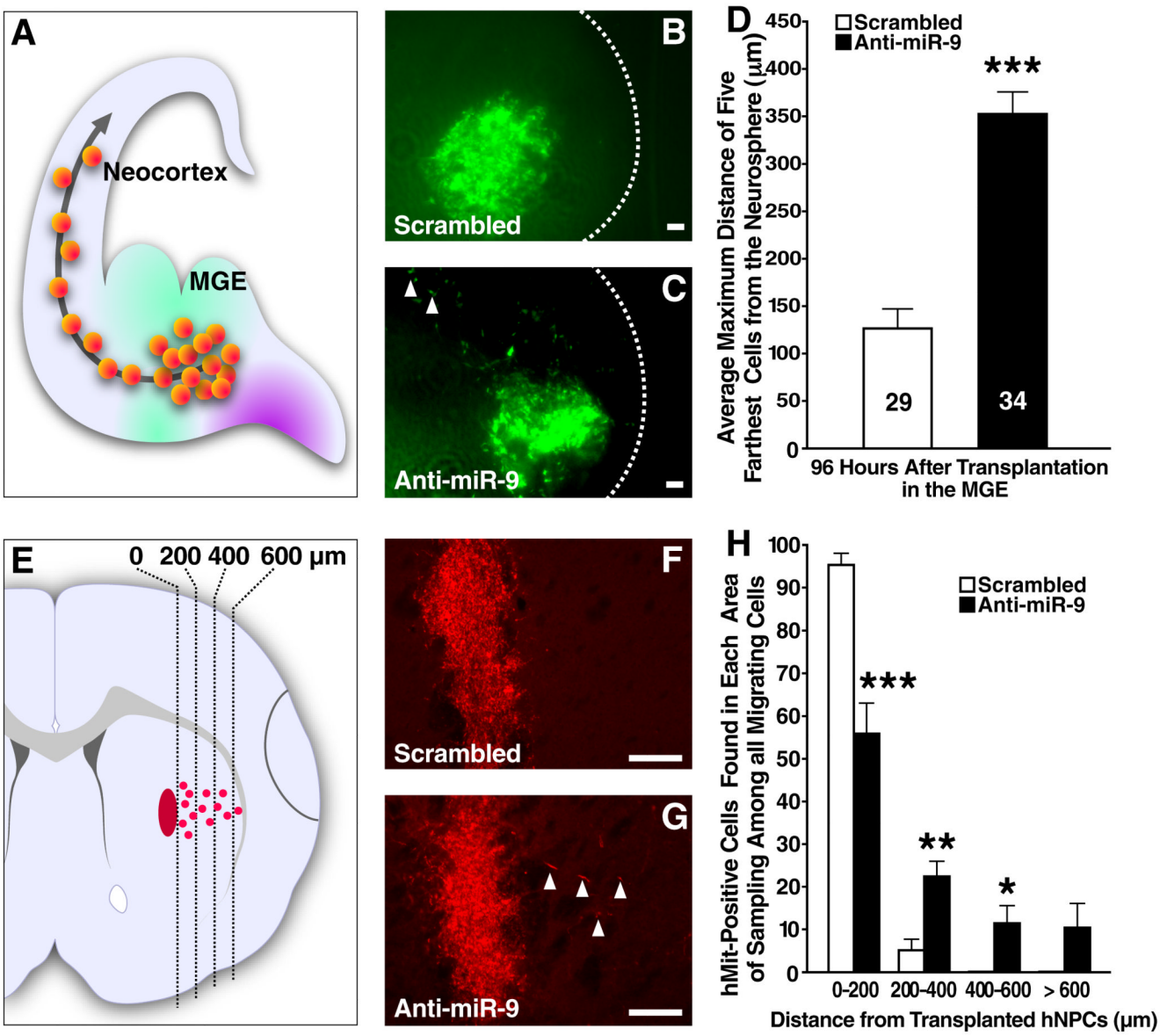

Figure 5. Migration of hNPCs In Embryonic Mouse Brain Slices and the Adult Brain of a Mouse Stroke Model

(A) A diagram of the brain in the E14.5 forebrain slice culture.

(B) Scrambled LNA probe-transfected neurospheres derived from hESCs were transplanted into the medial ganglionic eminence (MGE). Scale bars, 50 µm.

(C) Transplanted hESC-derived neurospheres with miR-9 knockdown in the MGE. The arrowheads indicate a few migrating hNPCs.

(D) Maximum distance of hNPC migration out of neurospheres. Values are the mean ± s.e.m. of the five longest migrations. The quantification method is described in Experimental Procedures. The numbers of transplanted neurospheres in one experiment are indicated in each column. This experiment was repeated two more times with similar results.

(E) Analysis of migration of transplanted hNPCs in the striatum toward areas of brain injury in a mouse model of stroke. hNPCs in different sampling areas (0–200, 201–400, 401–600,

NIH-PA Author Manuscript

NIH-PA Author Manuscript

NIH-PA Author Manuscript

and >600 μm away from the transplanted hNPCs) were counted in each mouse after staining with anti-human mitochondria antibody (hMit).

(F) hNPCs transfected with scrambled LNA probe remained largely at the injection site. Bar: 200 μm.

(G) Some anti-miR-9-transfected hNPCs migrated away from the injection site toward the injury site. The arrowheads indicate a few migrating hNPCs.

(H) Percentages of migrated hNPCs in each area (n = 8 mice per group). Values are mean ± s.e.m.. $*P < 0.05$, $**P < 0.01$, $***P < 0.001$.

See also Figures S5 and S6.

NIH-PA Author Manuscript

NIH-PA Author Manuscript

NIH-PA Author Manuscript

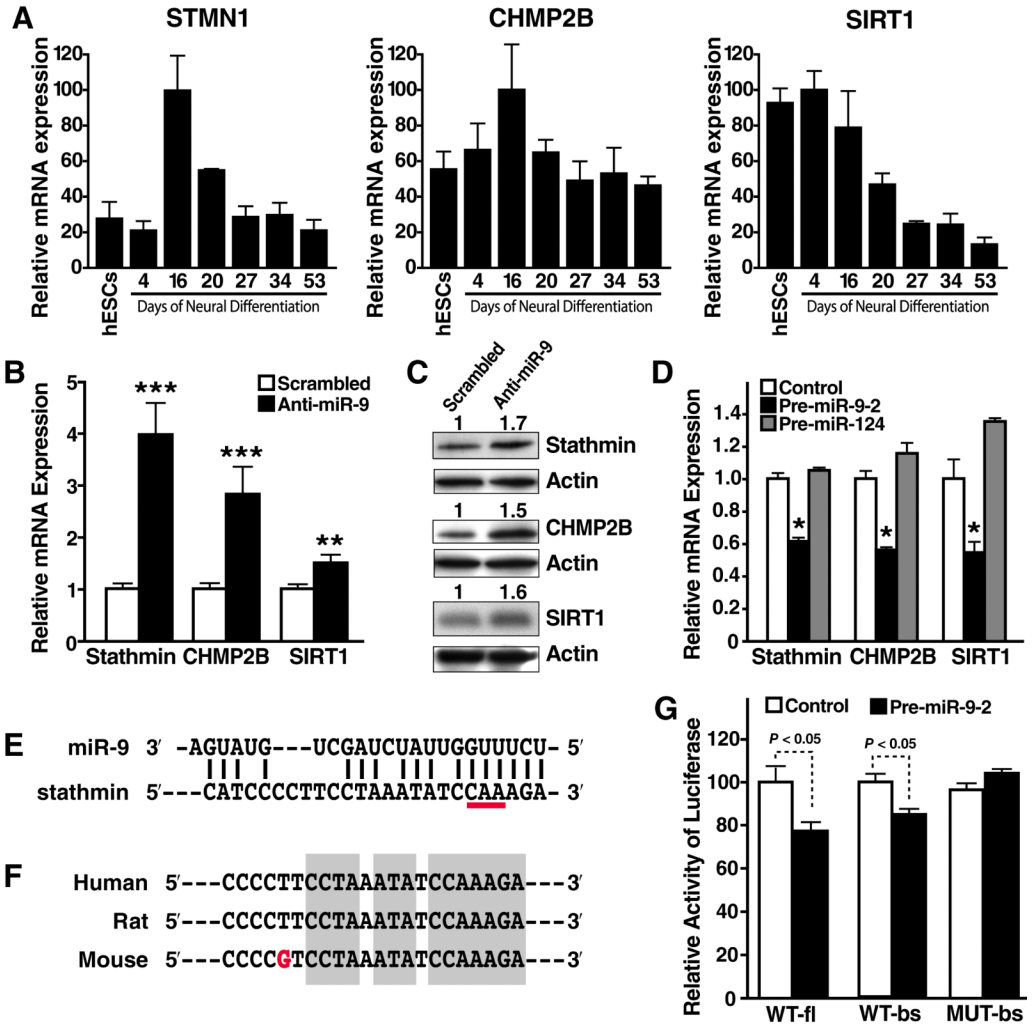

Figure 6. Identification of Stathmin as a Key mRNA Target Directly Regulated by MiR-9

(A) qRT-PCR analysis of expression profiles of miR-9 predicted mRNA targets during neuronal differentiation of hESCs. Expression was normalized to GADPH mRNA levels. Values are mean ± s.e.m. from at least three different cultures. See also Tables S1-S4.

(B) qRT-PCR analysis of mRNA expression levels of predicted targets of miR-9 in hNPCs 24 h after transfection with anti-miR-9 and scrambled control probes. Values are mean ± s.e.m. from five experiments, normalized to levels in control-transfected hNPCs.

(C) Western blot analysis demonstrating the expression levels of stathmin, CHMP2B, and SIRT1 in hNPCs 24 h after transfection with anti-miR-9. Actin served as a loading control. This analysis was repeated three times. Values are the average fold changes in the expression levels of these proteins.

(D) Expression levels of predicted targets of miR-9 in HEK293 cells 48 h after transfection with pre-miR-9-2. miR-124 precursor transfected HEK293 cells were used as a negative control.

(E) Sequence complementarity of a potential miR-9 binding site in the human stathmin 3′UTR. The three nucleotides mutated for the luciferase assay control experiment are underlined.

(F) Conserved nucleotides in human, rat and mouse stathmin 3′UTRs with complementarity to nucleotides 1–7, 9–11, and 12–15 of miR-9 (in gray).

NIH-PA Author Manuscript

NIH-PA Author Manuscript

NIH-PA Author Manuscript

(G) Relative luciferase activity of constructs containing the wildtype or mutant 3′UTR of stathmin cotransfected into HEK293 cells in the presence of control or pre-miR-9-2. Firefly luciferase activity was measured 48 h after transfection and normalized to the cotransfected Renilla luciferase construct. WT-fl: wildtype full-length stathmin 3′UTR. WT-bs: wildtype partial stathmin 3′UTR containing the putative miR-9 binding site. MUT-bs: partial stathmin 3′UTR with mutated seed region in the putative miR-9 binding site. For all panels, $*P < 0.05$. $**P < 0.01$. $***P < 0.001$.

See also Tables S1-4.

NIH-PA Author Manuscript

NIH-PA Author Manuscript

NIH-PA Author Manuscript

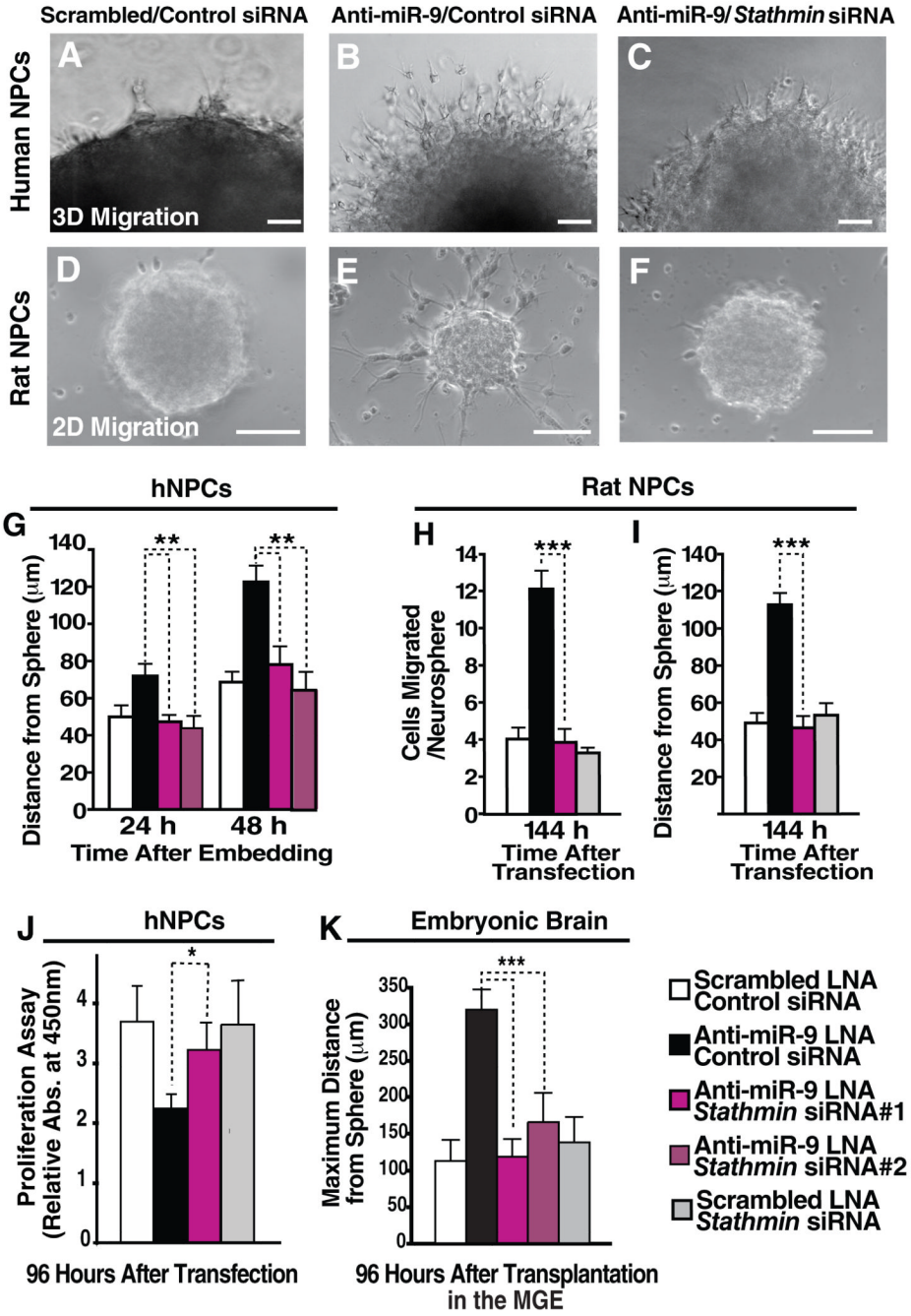

Figure 7. Stathmin Is an Essential Target of MiR-9 in Regulating NPC Migration and Proliferation

(A) and (D) Scrambled LNA and control siRNA transfected neurospheres.

(B) and (E) Anti-miR-9 LNA and control siRNA transfected neurospheres.

(C) and (F) Anti-miR-9 LNA and stathmin siRNA transfected neurospheres.

In panels A–C, neurospheres derived from hESCs were used, and images were obtained 4 days after transfection and 1 day after embedding into the 3D Matrigel.

In panels D–F, neurospheres derived from rat NPCs were used; images were obtained 6 days after transfection, and neurospheres were cultured on the top of plastic substrates.

In panels A–F, Scale bar, 100 μm.

NIH-PA Author Manuscript

NIH-PA Author Manuscript

NIH-PA Author Manuscript

(G) Average distance between the nucleus of most distal migrating hNPC from the neurosphere. Values are mean ± s.e.m. *n* >40 neurospheres. Key in panel K also applies to panels G–J.

(H) Number of rat NPCs that migrated away from neurospheres. Values are mean ± s.e.m. *n* >40 neurospheres.

(I) Average distance from the neurosphere to the nucleus of most distal migrating rat NPC. Values are mean ± s.e.m. n > 40 neurospheres.

(J) Partial suppression of stathmin expression by siRNA rescued the effect of loss of miR-9 activity on the proliferation of hNPCs in the WST-1 assay.

(K) Maximum distances that hNPCs migrated out of the neurospheres transplanted into the MGE. Values are mean ± s.e.m. n >15 neurospheres for each conditions. The experiment was repeated once with similar results. In all panels, $*P < 0.05$, $**P < 0.005$. $***P < 0.001$. See also Figure S7.